IEEE Access
Multidisciplinary ⋮ Rapid Review ⋮ Open Access Journal

Received December 30, 2020, accepted January 15, 2021, date of publication January 27, 2021, date of current version February 9, 2021.

Digital Object Identifier 10.1109/ACCESS.2021.3054944

Efficient Graphene Reconfigurable Reflectarray Antenna Electromagnetic Response Prediction Using Deep Learning

LI PING SHI, QING HE ZHANG, SHI HUI ZHANG, CHAO YI, AND GUANG XU LIU

College of Computer and Information, China Three Gorges University, Yichang 443002, China

Corresponding author: Qing He Zhang (zqh@ctgu.edu.cn)

This work was supported by the National Natural Science Foundation of China under Grant 61771008.

ABSTRACT Aiming at the time-consuming problem of the full-wave (FW) simulation of the scattering characteristics of the traditional graphene reconfigurable reflectarray antenna, a fast prediction method of electromagnetic (EM) response based on deep learning is proposed. The convolutional neural network (CNN) method in deep learning is effectively used in the research of this paper. This method first discretizes the input vector (patch geometry, chemical potential, frequency, incident angle, etc.) of the graphene reflectarray antenna, and then preprocesses the data into a two-dimensional image suitable for CNN training, and finally uses CNN to train the model instead of extensive FW simulation calculations, the EM response of the reflectarray antenna is calculated. The training results of three algorithms of support vector regression (SVR), radial basis function network (RBFN) and CNN are comprehensively compared. The experimental results show that CNN method has good performance and accuracy in the EM response prediction of the graphene reconfigurable reflectarray antenna, with an accuracy of over 99%, and can also save at least 99% of time.

INDEX TERMS Convolutional neural network (CNN), electromagnetic (EM) response, graphene, reconfigurable reflectarray antenna.

I. INTRODUCTION

The planar reflectarray antenna is a new type of high-gain antenna that uses a planar structure to replace the complex curved structure in the traditional parabolic antenna, which effectively reduces the design difficulty [1]. Microstrip reflectarray antenna is composed of feeder and microstrip antenna array. There are many microstrip reflection unit cells on the reflection plane, and different phase compensations can be realized by controlling the size of each unit cell without loading a complex feed network. The reflectarray antenna has broad application prospects [2]. The emergence of the reconfigurable reflectarray antenna enables it to change the basic working characteristics of the independent radiating unit cell to adapt to more diverse system requirements and complex and changeable application environments [3].

Graphene materials have good electrical conductivity, electrical conductance controllability, and plasmon characteristics in antenna design. Good conductivity makes it have better radiation than traditional metal antennas. By applying bias voltage, the chemical potential of graphene can be changed its surface conductivity, which in turn changes the value of graphene's surface impedance [4], [5]. Therefore, graphene materials have certain application potential in the research of reconfigurable antennas.

When the radiation patch of the reflectarray antenna unit cell uses graphene material, the electromagnetic (EM) response of the reflectarray antenna can be theoretically changed by changing the surface characteristics of graphene by applying voltage. There are many different methods for the analysis of reflectarray antennas. Since there is no simple closed-form expression, in view of the quasi-periodicity of this antenna, the commonly used method is the full-wave (FW) analysis method assuming partial periodicity [6]–[8]. The simulation of this periodic independent element can be proved to be very effective by the method of moments [6] or equivalent finite time domain analysis [7]. These methods can be used to calculate the EM response of any possible cell configuration, and the results are relatively accurate. Although there are many specific analysis methods for the

The associate editor coordinating the review of this manuscript and approving it for publication was Wei Xu.

scattering characteristics of reflectarray antennas, these methods require multiple boring and repetitive simulations of all possible unit cells, which have problems such as computational efficiency and large memory requirements. Therefore, reasonable and effective use of reflectarray antennas for high-efficiency communication, and efficient analysis and calculation of the periodic array scattering characteristics to reduce EM interference have become an urgent problem to be solved. In this context, the paper is of great significance for the efficient analysis and calculation of the EM response of the reflectarray antenna.

In recent years, the artificial intelligence method of machine learning has been widely used in the field of EM engineering, such as EM scattering [9], antenna diagnosis [10], parameter reconstruction [11], etc. Some effective machine learning methods [9], [12]–[14] for analyzing reflectarray antennas are also proposed. In [9], the author used support vector regression (SVR) to predict the EM response of single-layer ''Phoenix'' unit cell, but the network topology structure of SVR is relatively complex, and the computational efficiency is not particularly obvious.

At present, deep learning technology has been widely used in various fields such as language processing [15], image processing [16] and antenna design [17]. In this work, the author innovatively uses the convolutional neural network (CNN) in deep learning to predict the scattering characteristics of graphene reconfigurable reflectarray antenna elements in different polarization states (co-polarization and cross-polarization). Compared with traditional neural networks, CNN adopts a parameter sharing mechanism, which greatly reduces the number of network parameters, thereby effectively avoiding overfitting. In addition, CNN also uses a local connection method, which greatly improves network training efficiency and generalization ability.

The paper first discretizes the geometry of the graphene radiation patch, chemical potential, frequency and angle of the incident wave. Then use the FW simulation software (CST microwave studio) to simulate the reflectarray antenna element to obtain the CNN training data set. After offline training, the nonlinear regression model of the scattering coefficient matrix is established and the EM response of the graphene reconfigurable reflectarray antenna unit cell under different parameters is quickly predicted in real time. Finally, the prediction results of CNN are compared with the results obtained by the SVR method, the Radial Basis Function Network (RBFN) method, and the FW simulation method.

The paper is organized as follows. The second part provides an overview of the graphene surface conductivity and the radiation field of the reflectarray antenna. The third part explains the specific method of using CNN to predict the EM response of the graphene reconfigurable reflectarray antenna unit cell. The fourth part discusses the numerical results of CNN compared with other machine learning methods. The fifth part is a summary of the full text.

II. CHARACTERISTICS OF GRAPHENE RECONFIGURABLE REFLECTARRAY ANTENNA

Graphene materials can be represented by infinitely thin, two-dimensional, non-local anisotropic surface conductivity [4]. Assuming that there is no additional magnetic field, the surface conductivity of graphene becomes isotropic, which can be represented by $\sigma_s(\omega, \Gamma, T, \mu_c)$, where $\omega = 2\pi f$ is the radiation angular frequency, f is the frequency, $\Gamma = 1/(2\tau)$ is the electron scattering rate, τ is the propagation relaxation time (assuming $\tau = 1$ps [18]), T is the room temperature ($T = 300$K [5]), and μ_c is the chemical potential. The surface conductivity formula can be derived from the Kubo equation [19], [20]:

$$\begin{aligned}&\sigma_s(\omega, \Gamma, T, \mu_c)\\ &= \frac{je^2(\omega - j2\Gamma)}{\pi\hbar^2}\Big[\frac{1}{(\omega - j2\Gamma)^2}\int_0^\infty \varepsilon\Big(\frac{\partial f_d(\varepsilon)}{\partial\varepsilon} - \frac{\partial f_d(-\varepsilon)}{\partial\varepsilon}\Big)d\varepsilon\\ &\quad - \int_0^\infty \frac{f_d(-\varepsilon) - f_d(\varepsilon)}{(\omega - j2\Gamma)^2 - 4(\varepsilon/\hbar)^2}d\varepsilon\Big],\end{aligned} \tag{1}$$

where e is the electron charge, $\hbar = h/2\pi$ is the reduced Planck constant, ε is the energy, $f_d(\varepsilon) = (e^{(\varepsilon-\mu_c)/k_BT} + 1)^{-1}$ is the Fermi-Dirac distribution, and k_B is the Boltzmann constant. We can see from (1) that the conductivity of graphene is composed of two parts, one is expressed as the intra-band contribution of graphene (σ_{intra}), and the other is expressed as the inter-band contribution of graphene (σ_{inter}). In the case of low terahertz band (the center frequency in this work is $f_0 = 1$ Thz), only the intra-band contribution can be considered, so the surface conductivity can be approximately expressed as [18], [20], [21]:

$$\begin{aligned}&\sigma_s(\omega, \Gamma, T, \mu_c)\\ &\approx \sigma_{intra}(\omega, \Gamma, T, \mu_c)\\ &= -\frac{je^2k_BT}{\pi\hbar^2(\omega - j2\Gamma)}\left\{\frac{\mu_c}{k_BT} + 2\ln\left[\exp\left(-\frac{\mu_c}{k_BT}\right) + 1\right]\right\}.\end{aligned} \tag{2}$$

By applying bias voltage, the surface conductivity of graphene can be changed by changing its chemical potential, and thus the reconfigurability of the reflectarray antenna can be realized.

The microstrip reflectarray antenna is mainly composed of an illumination feeder and an array composed of many isolated microstrip patch unit cells, as shown in Fig. 1. The incident wave emitted by the feeder illuminates the reflective surface, and the incident phase of the incident wave to each reflectarray element is proportional to the distance from the center of the feeder to the element. After the different phases of each element are arranged, a specific phase shift distribution is formed on the reflective surface. The incident wave is compensated by different phases and then radiated, that is, the main beam is formed by superposition in a given direction [1].

Assuming that $N \times N$ reflectarray elements are periodically arranged on the plane, and the feeder radiates EM waves to the graphene patch to generate reflected and scattered

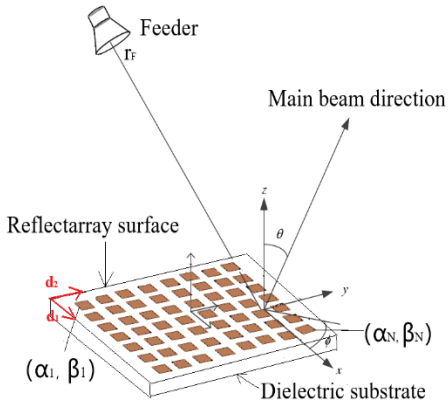

FIGURE 1. The structure of reflectarray antenna.

fields, the radiation field of every nth ($n = 1, \ldots, N^2$) graphene reflectarray antenna unit cells can be superimposed as follows [9], [12], [22]:

$$\begin{aligned}\boldsymbol{E}(\theta, \varphi; f) = \sum_{n=1}^{N^2} \{[\mathcal{R}(\theta_n, \varphi_n; f) + \mathcal{S}(\theta_n, \varphi_n; \mu_c, f, W_n, L_n)] \\ \cdot \boldsymbol{E}_F(\theta_n, \varphi_n; f) \exp(\mathrm{j}k_0(\alpha_n \sin\theta\cos\varphi \\ + \beta_n \sin\theta \sin\varphi))\},\end{aligned} \tag{3}$$

where θ_n and φ_n are the angles of incidence from the feeder to the nth patch, f is the working frequency, $\sin\theta\cos\varphi$ and $\sin\theta\sin\varphi$ are the direction cosines of the wave, α_n and β_n are the coordinates of the center of the nth patch element, $k_0 = (2\pi c_0)/f$ is the free-space wavenumber (c_0 being the speed of light), W_n and L_n are the width and length of the nth graphene patch $\mathcal{R}(\theta_n, \varphi_n; f) = \{R_{xy}(\theta_n, \varphi_n; f);\ x, y = \{\theta, \varphi\}\}$ is the plane wave reflection matrix, and $\mathcal{S}(\theta_n, \varphi_n; \mu_c, f, W_n, L_n) = \{S_{xy}(\theta_n, \varphi_n; \mu_c, f, W_n, L_n); x, y = \{\theta, \varphi\}\}$ is the scattering matrix, respectively, while

$$\begin{aligned}&\boldsymbol{E}_F(\theta_n, \varphi_n; f) \\ &= \frac{|\boldsymbol{r}_F|}{|\boldsymbol{r}_n - \boldsymbol{r}_F|} \frac{E_F(\theta_n, \varphi_n; f)}{E_F(0, 0; f)} \\ &\quad \times \exp(jk_0 |\boldsymbol{r}_n - \boldsymbol{r}_F| - |\boldsymbol{r}_F|)[\cos\varphi_n \hat{\boldsymbol{\theta}} + \sin\varphi_n \hat{\boldsymbol{\varphi}}]\end{aligned} \tag{4}$$

is the field pattern radiated by the feeder on the nth element, $\boldsymbol{r}_n$ is the location of the nth patch element, $\boldsymbol{r}_F$ is the feeder position, and $E_F(\theta, \varphi, f)$ is the element factor.

When the incident wave irradiates on the graphene patch, an additional scattering field is generated. According to (3), the incident field can be represented by the scattering coefficient matrix $\mathcal{S}(z), z \triangleq [W, L, \mu_c, f, \theta, \varphi]$, which indicates that the scattering coefficient $\mathcal{S}(z)$ is an important component for characterizing the graphene reconfigurable reflectarray antenna element. The output value $\mathcal{S}(z)$ is a function of input variables such as the geometric size of the graphene patch (W, L), the graphene chemical potential μ_c, the working frequency f, and the angle of the incident field (θ, φ). In this paper, the regression analysis of CNN is mainly used to replace the traditional FW simulation tool to obtain the alternative model, and then the predicted value $\hat{S}(z)$ of the scattering coefficient matrix is obtained to approximate the true value $\mathcal{S}(z)$, that is, $\hat{S}(z) \approx \mathcal{S}(z), z \in \mathbb{Z}(\mathbb{Z} \triangleq \{W \in [W_{\min}, W_{\max}]; L \in [L_{\min}, L_{\max}]; \mu_c \in [\mu_{c\,\min}, \mu_{c\,\max}]; f \in [f_{\min}, f_{\max}]; \theta \in [\theta_{\min}, \theta_{\max}]; \varphi \in [\varphi_{\min}, \varphi_{\max}]\})$.

III. USE CNN TO CHARACTERIZE GRAPHENE REFLECTARRAY ANTENNA ELEMENT

As a major research direction in deep learning [23], CNN is a feedforward multi-layer perceptron neural network, which mainly uses local receptive field and weight sharing mechanism to reduce the training parameters to a great extent [24], so that the training of deep network model can be realized. The CNN model is based on supervised learning, which can spontaneously extract data features from a large number of training samples, avoiding poor prediction results due to improper construction of features. In this paper, CNN is used instead of the traditional FW simulation tool to rapidly predict the EM response of the graphene reconfigurable reflectarray antenna element so as to improve the efficiency of antenna design and optimization.

The complex scattering coefficient of the graphene reflectarray antenna unit cell will change with different degrees of freedom, so the output of CNN is the complex scattering coefficient matrix of the antenna unit cell in the co-polarized and cross-polarized state, and the input is a 6- dimensional vector (i.e., 6 degrees of freedom) containing the width and length of the patch (W, L), the graphene chemical potential μ_c, the working frequency f, and the incident angle in spherical coordinates (θ, φ). As mentioned above, we need a sample set to train CNN, which is obtained by FW simulation. For this, we need to discretize each input parameter.

The width and length of the graphene patch are divided into I divisions respectively, so there are A ($A = i^2, i = 1, \ldots, I$, W_i represents patch width, L_i represents patch length) total of possible antenna unit cells. In addition, we need divide the graphene chemical potential into B divisions ($\mu_{c(b)}, b = 1, \ldots, B$), C divisions for the working frequency ($f_c, c = 1, \ldots, C$), D divisions for the elevation angle ($\theta_d, d = 1, \ldots, D$), and E divisions for the azimuth angle ($\varphi_e, e = 1, \ldots, E$). In this case, we need to use the FW method to perform $R = A \times B \times C \times D \times E$ different simulations to establish a training sample set. The time required for one FW calculation for each antenna element is $T_{\text{sin}}^{\text{FW}} \approx 180$s. If the input parameters are more finely discrete, assuming there are $R = 5 \times 10^4$ antenna elements, the required time is $T_{\text{all}}^{\text{FW}} \approx R \times T_{\text{sin}}^{\text{FW}} = 9 \times 10^6$s (about 105 days). Although using FW simulation to perform multiple repetitive calculations can simply and accurately obtain the EM response of the graphene reflectarray antenna unit cell, this process is not only time-consuming and labor-intensive, but also requires a lot of storage space. For solving the problem of data storage and computing time, this paper proposes a deep learning method based on CNN. To this end, a data sample $Q \triangleq \{z_r, S(z_r); z_r \triangleq [W_i, L_i, \mu_{c(b)}, f_c, \theta_d, \varphi_e], r = 1, \ldots, R\}$ is established by FW calculation of the above A antenna

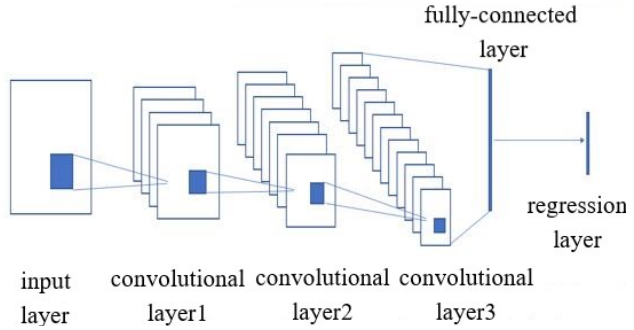

FIGURE 2. Architecture of the convolutional neural network.

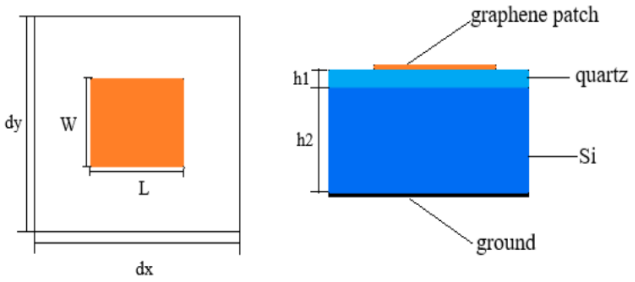

FIGURE 3. Schematic diagram of reflectarray antenna unit cell containing two layers of dielectric substrate.

elements under different chemical potentials, working frequencies and incident angles, and then a certain number of samples are randomly selected from the R data samples as the training set for CNN to learn.

This paper uses the deep learning toolbox that comes with MATLAB2020 to build a CNN model, which is mainly composed of input layer, convolutional layer, fully-connected layer and regression layer, as shown in Fig. 2.

As the common CNN is mainly used to extract image features and accept data in matrix form for operation, the data is matrixed before entering the input layer. Since the transformed data matrix itself has relatively low dimensionality, there is no need to perform additional dimensionality reduction operations on the data, so the step size of all convolutional layers in CNN is set to 1, and the pooling layer that plays the role of reducing the feature dimension in the neural network is removed. A batch normalization layer is added behind each convolutional layer, and LeakyReLU activation function is accessed behind the batch normalization layer. In addition, the dropout layer is added in front of the fully-connected layer to prevent overfitting when the number of iterations increases. In the process of training the network, the optimization algorithm of mini-batch gradient descent (MBGD) is used. The network performs 40 rounds of training, sets the initial learning rate to 0.001, and reduces the learning rate after 30 rounds of training. Finally, trainNetwork is used to create a network, and then a prediction model of the EM response of the graphene reconfigurable reflectarray antenna unit cell is obtained.

In order to verify the accuracy and effectiveness of the method in this paper, the calculation formula of error index and calculation efficiency is given below to quantitatively evaluate the performance of the proposed method. The magnitude and phase errors ξ_1 and ξ_2 of the scattering coefficient matrix $S(z)$ are defined as follows [9], [12]:

$$\xi_1 \triangleq \frac{1}{M}\sum_{m=1}^{M}\frac{\left\|\hat{S}^{\mathrm{CNN}}(z_m)-S(z_m)\right\|^2}{\|S(z_m)\|^2}, \tag{5}$$

where S is the accurate scattering coefficient matrix calculated by FW method, and $\hat{S}$ is the predicted, $\|\cdot\|$ is the norm of matrix 2, and M is the number of samples in the test set.

$$\xi_2 \triangleq \frac{1}{4M}\sum_{m=1}^{M}\left|\frac{1}{\pi}\arg\left[\frac{\hat{S}^{\mathrm{CNN}}(z_m)}{S(z_m)}\right]\right|^2, \tag{6}$$

where the normalization of π indicates that the phase is actually expressed in radians, and the coefficient $1/4$ refers to the four entries of the scattering matrix. Another evaluation factor, computational efficiency, that is, the time saved by CNN compared with FW simulation, is defined as follows [9]:

$$\Delta T^{\mathrm{CNN}} \triangleq 1-\left|\frac{T^{\mathrm{CNN}}_{\mathrm{train}}+T^{\mathrm{CNN}}_{\mathrm{test}}}{T^{\mathrm{FW}}}\right|, \tag{7}$$

where $T^{\mathrm{FW}} \triangleq M \times T^{\mathrm{FW}}_{\mathrm{sin}}$ represents the time required to calculate the FW simulation of M test sets, $T^{\mathrm{CNN}}_{\mathrm{train}}$ represents the time required for the CNN training process, and $T^{\mathrm{CNN}}_{\mathrm{test}}$ (can be ignored) represents the time required for the CNN test process.

IV. NUMBERICAL RESULTS

The structure of the common basic reflectarray antenna unit cell includes square patch, square ring, round patch, ring, etc. Other complex reflectarray antenna unit cell structures are generally realized by arbitrarily combining basic structures, adding or removal of part of the basic structures. As shown in Fig. 3, the rectangular patch is taken as the research object in this paper, and the graphene patch with a thickness of 38 nm is printed on a two-layer dielectric substrate ($\mathrm{d}x = \mathrm{d}y = \lambda_0/10$, λ_0 is the wavelength at center frequency f_0). The first dielectric layer is a high-resistance quartz layer with a dielectric constant of 3.78 and a thickness of 50 nm. The second layer is made of low resistance silicon, which can maintain a uniform level with the metal floor under applied voltage. The silicon wafer has a dielectric coefficient of 11.9 and a thickness of 25 μm.

In this work, suppose the graphene patch size W_i, $L_i \in [8\,\mu\mathrm{m}, 14\,\mu\mathrm{m}]$, the graphene chemical potential $\mu_{c(b)} \in [0\,\mathrm{eV}, 1\,\mathrm{eV}]$, the working frequency $f_c \in [0.8\,\mathrm{THz}, 1.1\,\mathrm{THz}]$, the elevation angle $\theta \in [0\,\mathrm{deg}, 40\,\mathrm{deg}]$, and the azimuth angle $\varphi \in [0\,\mathrm{deg}, 45\,\mathrm{deg}]$. $R = 4 \times 4 \times 6 \times 4 \times 5 \times 4 = 7680$ data samples are obtained by discrete sampling of the parameters of these antenna elements. From the above 7680 samples,

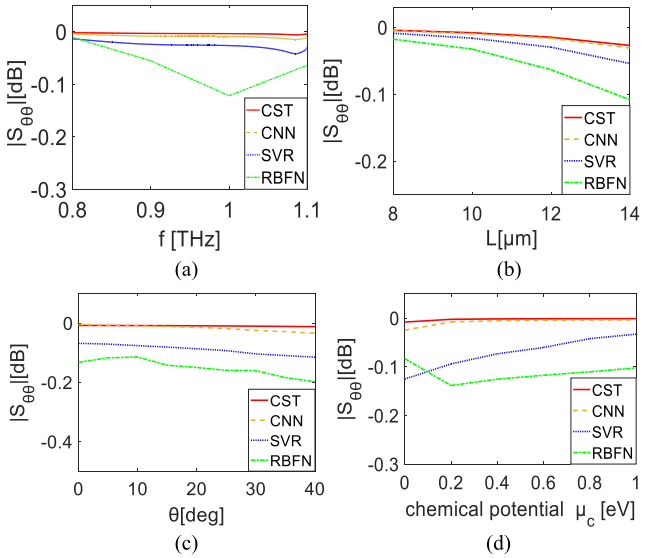

FIGURE 4. The magnitude of $S_{\theta\theta}(z)$ varies with frequency f, element size L, incident angle θ, and chemical potential μ_c.

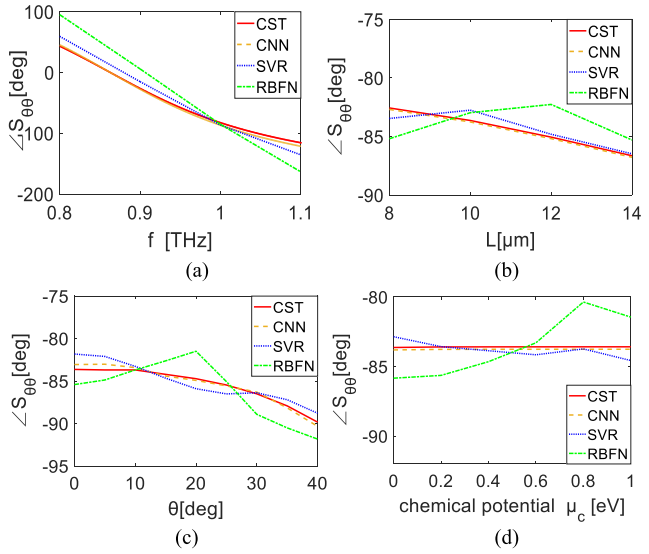

FIGURE 5. The phase of $S_{\theta\theta}(z)$ varies with frequency f, element size$L$, incident angle θ, and chemical potentialμ_c.

6000 samples are randomly selected as the training set, and the rest are used as the testing set.

Although CNN is a multi-input and multi-output system, the author has confirmed that the single output has a shorter training time than the multi-output, and can control the network topology more accurately. After the equivalent model is established by using CNN, several data not belonging to the training sample are randomly selected from vector space $\mathbb{Z}$ as validation sets to verify the effectiveness of the proposed method.

Fig. 4(a) shows the variation curve of the magnitude of $S_{\theta\theta}(z)$ based on CNN with the working frequency f, and also shows the calculation results based on SVR, RBFN, and FW simulation, where $W = 9\,\mu$m, $L = 10\,\mu$m,

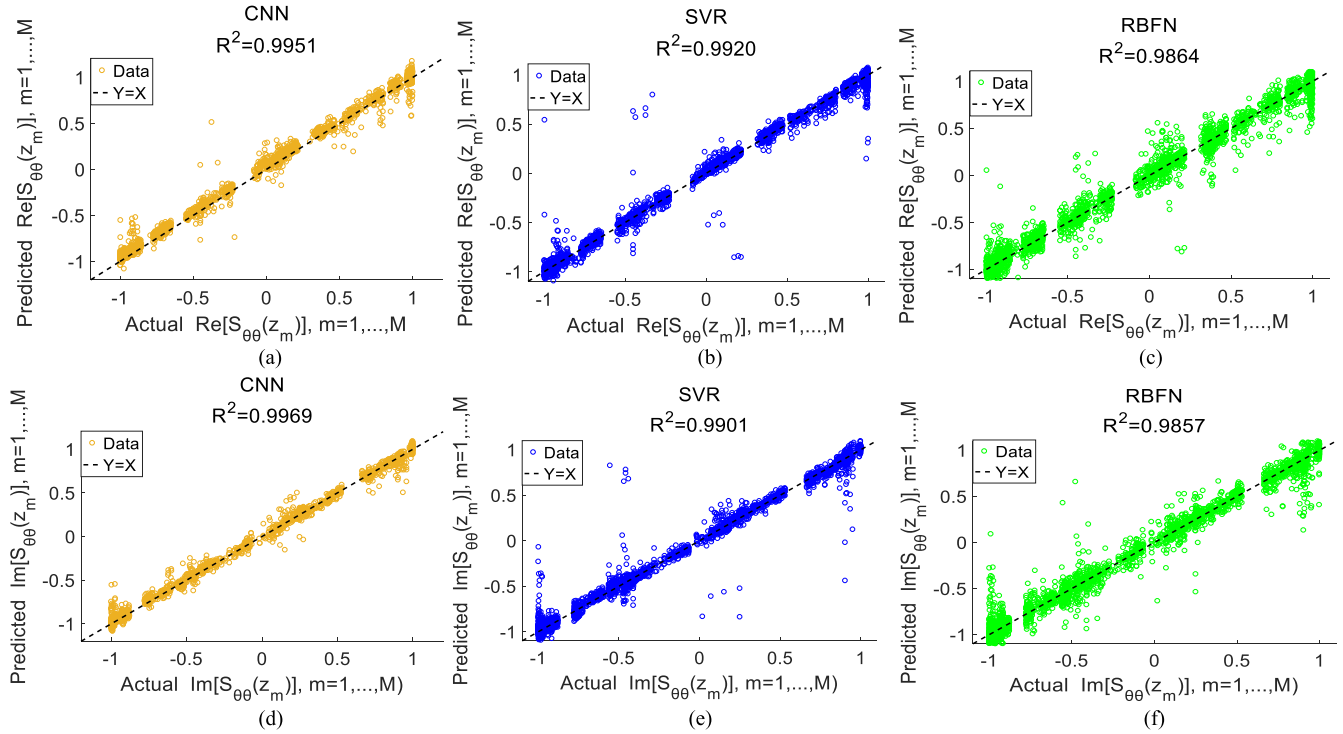

FIGURE 6. Actual versus estimated values of (a)-(c) Re$[S_{\theta\theta}(z_m)]$, $m = 1, \ldots, M$, and (d)-(f) Im$[S_{\theta\theta}(z_m)]$, $m = 1, \ldots, M$ when using (a) and (d) CNN, (b) and (e) SVR, and (c) and (f) RBFN prediction methods.

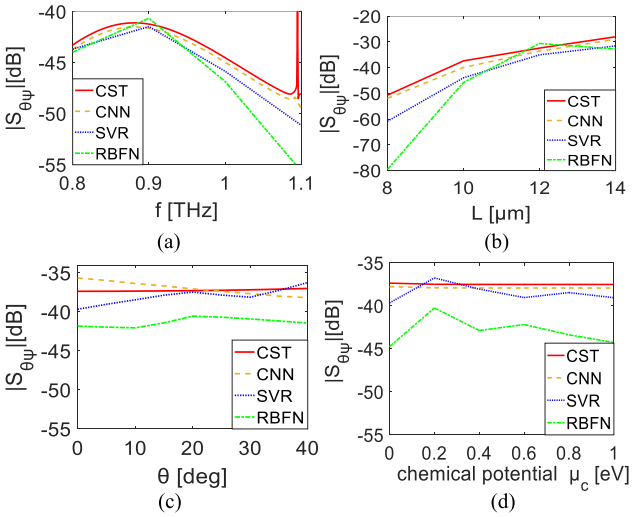

FIGURE 7. The magnitude of $S_{\theta\varphi}(z)$ varies with frequency f, element size$L$, incident angleθ, and chemical potentialμ_c.

$\mu_c = 0\,\text{eV}, \theta = 0\,\text{deg}, \varphi = 45\,\text{deg}$. Fig. 4(b) shows the variation curve of $S_{\theta\theta}(z)$ magnitude with the patch side length L, where $f = 1\,\text{THz}$ and other parameters remain unchanged. Analogously, Fig. 4(c) and (d) show the variation of co-polarization component $S_{\theta\theta}(z)$ magnitude with the incident angle θ and chemical potential μ_c, respectively. We can observe from the plots that the results obtained by CNN are very close to the true values, and are significantly better than SVR and RBFN in predicting the scattering magnitude.

Under the same conditions, Fig. 5 shows the phase of $S_{\theta\theta}(z)$ changes with frequency f, patch size L, incident angle θ and chemical potential μ_c.

As we expected, the difference between CNN and FW simulation is very small, the maximum difference from the FW simulation does not exceed 7 deg.

Fig. 6 shows the scatter plots of the real parts $\text{Re}[S_{\theta\theta}(z_m)], m = 1, \ldots, M$ and the imaginary parts $\text{Im}[S_{\theta\theta}(z_m)], m = 1, \ldots, M$ of the complex scattering coefficient matrix $\mathcal{S}(z), z \triangleq [\theta, \varphi; \mu_c, f, W, L]$, where $Y = X$ represents the ideal bisector. The figures show that the scatter distribution of CNN is closer to the ideal bisector than that of SVR and RBFN, which can also be well proved by the correlation coefficient R^2 shown in plots. The higher R^2, the stronger the correlation and the higher the accuracy. Plus, from the perspective of quantitative analysis, according to (5) and (6), the prediction errors of the $S_{\theta\theta}(z)$ magnitude and phase of the three methods of CNN, SVR, and RBFN can be obtained respectively. They are $\xi_1^{\text{CNN}} = 0.0091$, $\xi_2^{\text{CNN}} = 0.0113$, $\xi_1^{\text{SVR}} = 0.0162$, $\xi_2^{\text{SVR}} = 0.0364$, $\xi_1^{RBFN} = 0.0533$, and $\xi_2^{\text{RBFN}} = 0.0602$ respectively.

In order to further prove the effectiveness of the method proposed in this paper, Fig. 7 and Fig. 8 show the variation of the magnitude and phase of the cross-polarized component $S_{\theta\varphi}(z)$ with frequency f, graphene patch size L, incident angle θ and graphene chemical potential μ_c, respectively. Fig. 7 and Fig. 8 take the same input parameters as Fig. 4 and Fig. 5. Fig. 9 also shows a scatter plot of the real and imaginary parts of the complex number $S_{\theta\varphi}(z)$. Considering the symmetrical characteristics of the reflectarray antenna element, although the prediction accuracy of the cross-polarization component is slightly inferior to that of the co-polarization component, we can see from Fig. 7-Fig. 9 that CNN model can still more accurately match the FW simulation, regardless of the magnitude or phase, although the cross-polarized coefficient presents a highly nonlinear behavior.

According to (5) and (6), the magnitude and phase errors of the cross-polarization coefficient $S_{\theta\varphi}(z)$ can also be obtained. They are $\xi_1^{\text{CNN}} = 0.0285$, $\xi_2^{\text{CNN}} = 0.0318$, $\xi_1^{\text{SVR}} = 0.1166$, $\xi_2^{\text{SVR}} = 0.0963$, $\xi_1^{RBFN} = 0.1417$, and $\xi_2^{\text{RBFN}} = 0.1532$ respectively.

In terms of calculation efficiency, the design process of each graphene reflectarray antenna is independent of each other. It is traditionally done by using commercial FW simulation software. Changing the parameters of different antennas requires multiple calls to simulation software tools. For a very large and complex antenna, it may require hundreds or even thousands of calls to the tool, and it may take several hours to complete the design of an antenna. We can see that the use of machine learning methods to accelerate the design and analysis of antennas is an inevitable trend of development. This work is performed on a desktop computer with an Intel Core i7-7700 CPU at 3.6GHz. The time to complete a FW calculation is $T_{\text{sin}}^{\text{FW}} \approx 180$s. According to (7), $\Delta T^{\text{CNN}} = 0.996$, which saves 99.6% of time compared with the FW solver, significantly speeds up the prediction of the EM response of the graphene reconfigurable reflectarray

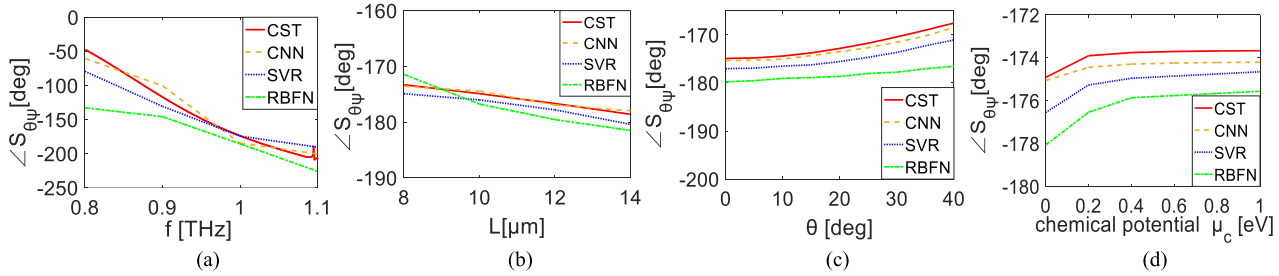

FIGURE 8. The phase of $S_{\theta\varphi}(z)$ varies with frequency f, element size$L$, incident angle θ, and chemical potentialμ_c.

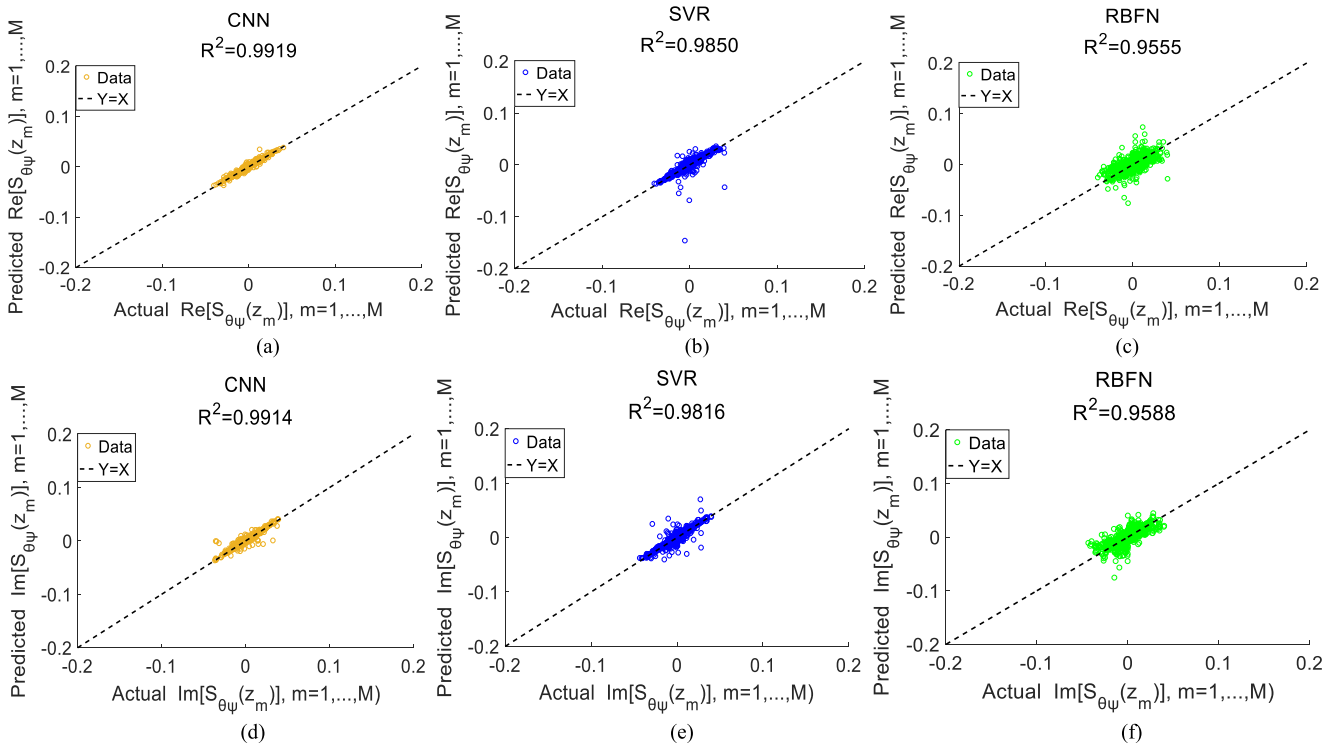

FIGURE 9. Actual versus estimated values of (a)-(c) Re$[S_{\theta\varphi}(z_m)]$, $m = 1, \ldots, M$, and (d)-(f) Im$[S_{\theta\varphi}(z_m)]$, $m = 1, \ldots, M$ when using (a) and (d) CNN, (b) and (e) SVR, and (c) and (f) RBFN prediction methods.

antenna. $\Delta T^{\mathrm{SVR}} = 0.64$ and $\Delta T^{\mathrm{RBFN}} = 0.87$ can also be obtained according to (7), that is, the time saved by using SVR and RBFN is 64% and 87% respectively.

V. CONCLUSION

In this paper, a new method to characterize the reflectarray antenna element is presented. The radiation patch of the antenna element is made of graphene materials to realize the reconfigurability of the reflectarray antenna. By taking the patch geometry, chemical potential, incident wave frequency and angle as input, the EM response of the graphene reconfigurable reflectarray antenna element is fully characterized by using CNN. In addition, according to (5)-(7), compared with the prediction performance of SVR and RBFN, CNN is superior to SVR and RBFN in terms of calculation accuracy and calculation efficiency. Regardless of the co-polarization component or the cross-polarization component, the prediction accuracy and calculation efficiency of CNN reached 99%, which verified the effectiveness of the method proposed in this paper. At the same time, it also proves that deep learning has greater application prospects in the field of antennas.

REFERENCES

[1] J. Huang and J. A. Encinar, *Reflectarray Antennas*. Piscataway, NJ, USA: Wiley, 2008.

[2] H. Yang, X. Chen, F. Yang, S. Xu, X. Cao, M. Li, and J. Gao, "Design of resistor-loaded reflectarray elements for both amplitude and phase control," *IEEE Antennas Wireless Propag. Lett.*, vol. 16, pp. 1159–1162, 2017, doi: 10.1109/LAWP.2016.2626318.

[3] S. V. Hum, M. Okoniewski, and R. J. Davies, "Modeling and design of electronically tunable reflectarrays," *IEEE Trans. Antennas Propag.*, vol. 55, no. 8, pp. 2200–2210, Aug. 2007.

[4] A. H. C. Neto, F. Guinea, N. M. R. Peres, K. S. Novoselov, and A. K. Geim, "The electronic properties of graphene," *Rev. Mod. Phys.*, vol. 81, no. 1, pp. 109–162, 2009.

[5] K. Novoselov, Z. Jiang, Y. Zhang, and S. Morozov, "Room-temperature quantum Hall effect in graphene," *Science*, vol. 315, no. 5817, p. 1379, Mar. 2007.

[6] D. R. Prado, M. Arrebola, M. R. Pino, R. Florencio, R. R. Boix, J. A. Encinar, and F. Las-Heras, "Efficient crosspolar optimization of shaped-beam dual-polarized reflectarrays using full-wave analysis for the antenna element characterization," *IEEE Trans. Antennas Propag.*, vol. 65, no. 2, pp. 623–635, Feb. 2017.

[7] R. T. Lee and G. S. Smith, "An alternative approach for implementing periodic boundary conditions in the FDTD method using multiple unit cells," *IEEE Trans. Antennas Propag.*, vol. 54, no. 2, pp. 698–705, Feb. 2006.

[8] R. Chiniard, A. Barka, and O. Pascal, "Hybrid FEM/floquet modes/PO technique for multi-incidence RCS prediction of array antennas," *IEEE Trans. Antennas Propag.*, vol. 56, no. 6, pp. 1679–1686, Jun. 2008.

[9] L. Shi, Q. Zhang, and S. Zhang, "Application of machine learning method to the prediction of EM response of reflectarray antenna elements," in *Proc. Photon. EM Res. Symp.*, Xiamen, China, 2019, pp. 2671–2676.

[10] C. Shan, X. Chen, H. Yin, W. Wang, G. Wei, and Y. Zhang, "Diagnosis of calibration state for massive antenna array via deep learning," *IEEE Wireless Commun. Lett.*, vol. 8, no. 5, pp. 1431–1434, Oct. 2019.

[11] H. Ming Yao, W. E. I. Sha, and L. Jiang, "Two-step enhanced deep learning approach for electromagnetic inverse scattering problems," *IEEE Antennas Wireless Propag. Lett.*, vol. 18, no. 11, pp. 2254–2258, Nov. 2019.

[12] M. Salucci, L. Tenuti, G. Oliveri, and A. Massa, "Efficient prediction of the EM response of reflectarray antenna elements by an advanced statistical learning method," *IEEE Trans. Antennas Propag.*, vol. 66, no. 8, pp. 3995–4007, Aug. 2018.

[13] D. R. Prado, J. A. Lopez-Fernandez, M. Arrebola, and G. Goussetis, "Efficient shaped-beam reflectarray design using machine learning techniques," in *Proc. 48th Eur. Microw. Conf. (EuMC)*, Madrid, Spain, Sep. 2018, pp. 1545–1548.

[14] V. Richard, R. Loison, R. Gillard, H. Legay, and M. Romier, "Loss analysis of a reflectarray cell using ANNs with accurate magnitude prediction," in *Proc. 11th Eur. Conf. Antennas Propag. (EUCAP)*, Paris, France, Mar. 2017, pp. 2402–2405.
[15] S. K. A. Fahad and A. E. Yahya, "Inflectional review of deep learning on natural language processing," in *Proc. Int. Conf. Smart Comput. Electron. Enterprise (ICSCEE)*, Shah Alam, Malaysia, Jul. 2018, pp. 1–4.
[16] O. Ronneberger, P. Fischer, and T. Brox, "U-net: Convolutional networks for biomedical image segmentation," in *Proc. Med. Image Comput. Comput.-Assist. Intervent*, 2015, pp. 234–241.
[17] A. M. Alzahed, S. M. Mikki, and Y. M. M. Antar, "Nonlinear mutual coupling compensation operator design using a novel electromagnetic machine learning paradigm," *IEEE Antennas Wireless Propag. Lett.*, vol. 18, no. 5, pp. 861–865, May 2019.
[18] Y. Yuan, Y. N. Xie, and X. Li, "Frequency-tunable graphene patch antenna in terahertz regime," *Acta Opt. Sinica*, vol. 38, no. 2, pp. 278–284, Oct. 2018.
[19] L. Wang, B. F. He, and Q. F. Sun, "Studies on a novel low-profile graphene THz antenna," *J. Micro.*, vol. 31, no. 1, pp. 17–21, Feb. 2015.
[20] K. Niu, P. Li, Z. Huang, L. Jun Jiang, and H. Bagci, "Numerical methods for electromagnetic modeling of graphene: A review," *IEEE J. Multiscale Multiphys. Comput. Techn.*, vol. 5, no. 4, pp. 44–58, Mar. 2020, doi: 10.1109/JMMCT.2020.2983336.
[21] V. P. Gusynin, S. G. Sharapov, and J. P. Carbotte, "Magneto-optical conductivity in graphene," *J. Phys., Condens. Matter*, vol. 19, no. 2, pp. 249–264, Jan. 2007.
[22] D. M. Pozar, S. D. Targonski, and H. D. Syrigos, "Design of millimeter wave microstrip reflectarrays," *IEEE Trans. Antennas Propag.*, vol. 45, no. 2, pp. 287–296, Feb. 1997.
[23] Z. J. Sun, L. Xue, Y. M. Xu, and Z. Wang, "Overview of deep learning," *Appli. Res. Comput.*, vol. 29, no. 8, pp. 2806–2810, Aug. 2012.
[24] Y. Lecun, L. Bottou, Y. Bengio, and P. Haffner, "Gradient-based learning applied to document recognition," *Proc. IEEE*, vol. 86, no. 11, pp. 2278–2324, Nov. 1998.

LI PING SHI was born in Lu'an, Anhui, China, in 1994. She received the bachelor's degree in communication engineering from the College of Electrical Engineering, Anhui Polytechnic University, Wuhu, China, in 2018. She is currently pursuing the master's degree in information and communication engineering with the College of Computer and Information, China Three Gorges University, Yichang, China. Her research interest includes antenna theory and design.

QING HE ZHANG received the B.S. degree in physics from Central China Normal University, Wuhan, China, in 1992, and the Ph.D. degree in radio physics from Wuhan University, Wuhan, in 2007.

From 2007 to 2014, he was an Associate Professor of electromagnetic fields with the Department of Physics, China Three Gorges University, Yichang, China, where he has been a Professor of electromagnetic fields with the Department of Computer and Information, since 2015. He is the author/a coauthor of more than 70 peer-reviewed papers in international journals and conferences. His research interests include electromagnetic direct and inverse problems, antenna array design and synthesis, radar signal processing, and theory/applications of optimization techniques and machine learning methods to electromagnetic engineering problems.

SHI HUI ZHANG was born in Linyi, Shandong, China, in 1995. She received the bachelor's degree in electronic information engineering from the College of Physics and Electrical Engineering, Linyi University, Linyi, in 2018. She is currently pursuing the master's degree in information and communication engineering with the College of Computer and Information, China Three Gorges University, Yichang, China. Her primary research interest includes DOA.

CHAO YI was born in Wuhan, Hubei, China, in 1990. He received the B.E. degree in electronic information science and technology from Hubei Minzu University, Enshi, China, in 2013. He is currently pursuing the Master of Engineering degree in electromagnetic inverse scattering theory with China Three Gorges University, Yichang, China.

GUANG XU LIU was born in Hebi, Henan, China, in 1996. He received the B.E. degree in communication engineering from the Zhengzhou University of Light Industry, Zhengzhou, China, in 2017. He is currently pursuing the M.E. degree with China Three Gorges University, Yichang, China. His research interest includes transmission.